Progress In Electromagnetics Research, Vol. 156, 1–12, 2016

Metamaterial Antenna Arrays for Improved Uniformity of Microwave Hyperthermia Treatments

David Vrba[1, *], Dario B. Rodrigues[2], Jan Vrba[1], and Paul R. Stauffer[2]

Abstract—Current microwave hyperthermia applicators are not well suited for uniform heating of large tissue regions. The objective of this research is to identify an optimal microwave antenna array for clinical use in hyperthermia treatment of cancer. For this aim we present a novel 434 MHz applicator design based on a metamaterial zeroth order mode resonator, which is used to build larger array configurations. These applicators are designed to effectively heat large areas extending deep below the body surface and in this work they are characterized with numerical simulations in a homogenous muscle tissue model. Their performance is evaluated using three metrics: radiation pattern-based Effective Field Size (EFS), temperature distribution-based Therapeutic Thermal Area (TTA), and Therapeutic Thermal Volume (TTV) reaching 41–45°C. For 2×2 and 2×3 array configurations, the EFS reaching $> 25\%$ of maximum SAR in the 3.5 cm deep plane is 100% and 91% of the array aperture area, respectively. The corresponding TTA for these arrays is 95% and 86%, respectively; and the TTV attaining > 41°C is over 85% of the aperture area to a depth of over 3 cm in muscle, using either array configuration. With theoretical heating performance exceeding that of existing applicators, these new metamaterial zero order resonator arrays show promise for future applications in large area superficial hyperthermia.

1. INTRODUCTION

Hyperthermia is a cancer treatment technique used in multimodal therapies that involves raising tumor temperature within a narrow range of 41–45°C for about one hour. Numerous hyperthermia clinical studies have shown an effective thermal enhancement of both radiation and chemotherapy without undue normal tissue damage [2–4]. These studies concluded that for a successful hyperthermia treatment it is essential to heat the entire tumor volume and that current electromagnetic hyperthermia applicators are not well suited for heating large regions of tissue overlying contoured anatomy. Typical applicators consist of planar waveguide structures that generate an electric field (E-field) local maximum centrally in the guided wave structure which results in excessive heating under the middle of the aperture and reduced heating closer to the aperture perimeter These planar structures are usually poorly coupled to the irregular tissue surface reducing wave penetration and the ability to heat deeper than 3 cm. To overcome these limitations we present a new applicator based on a novel metamaterial zeroth order mode (MTM-ZOR) antenna. This antenna can be arranged in appropriately spaced array configurations that effectively heat large areas extending deep inside the body [5].

The concept of MTM was first introduced by Veselago in 1968 [6] when he hypothesized the existence of materials whose permittivity (ε) and permeability (μ) were simultaneously negative. For plane waves propagating in these negative index materials, the electric field, magnetic field and wave vector form a left-handed triplet of vectors, which contrasts with traditional right-hand materials where $\varepsilon > 0$ and $\mu > 0$. However, the existence of left-handed metamaterials was not confirmed experimentally until

Received 27 January 2016, Accepted 31 March 2016, Scheduled 13 April 2016

* Corresponding author: David Vrba (david.vrba@fbmi.cvut.cz).

[1] Faculty of Biomedical Engineering, Czech Technical University in Prague, Zikova 4, Prague 166 36, Czech Republic. [2] Radiation Oncology Department, Thomas Jefferson University, Bodine Cancer Center, 111 S. 11th. St. Philadelphia, PA 19107, USA.

37 years later by a research group at the University of California, San Diego [7]. Since then, several electromagnetic (EM) radiating structures based on the MTM principle have been introduced, but effective implementation of such antennas has been limited due to poor radiation efficiency. The main issue limiting radiation efficiency has been antenna geometry, where currents flowing on the dominant radiating parts are canceled by currents flowing in the ground plane [8]. MTM antennas with improved radiation efficiency were investigated by Polivka and Vrba [9] who described a novel design modified by increasing the distance between the dominant radiating parts and the ground plane.

MTM lenses have been proposed as hyperthermia microwave applicators to treat superficial cancers [10, 11]. Our group was the first to investigate the conceptually different MTM-ZOR antennas for use in cancer treatment. In previous work, we adapted MTM-ZOR radiators for coupling to tissue and presented the first MTM-ZOR microwave antennas intended for use in hyperthermia [12]. The applicators have shown potential to improve the homogeneity of EM power deposition and effective penetration depth of EM waves in human tissue. As a result of the spatial arrangement of MTM resonators, the radiation pattern approximates an almost perfect electromagnetic plane wave as it emerges from the aperture and propagates into the target tissue region. This improvement in wave propagation optimizes the homogeneity of power deposition under the aperture with corresponding improvement in uniformity of temperature distribution throughout the target volume.

Since the physical length of ZOR resonators is independent of wavelength, electrically small MTM applicators can be constructed from one or more ZOR resonators. This allows us to design applicators with dimensions matching the clinical requirement. In addition, these applicators can radiate efficiently without having their inner structure filled with high dielectric material (e.g., water) like many traditional microwave applicators [13, 14]. The reduction of total water amount in a hyperthermia system reduces applicator bulk, and facilitates compatibility with magnetic resonance imaging equipment, which is increasingly being used for 3D thermal imaging to monitor and control hyperthermia treatments [15].

Our group recently introduced three different types of MTM-ZOR applicators that operate at 434 MHz [16]. Two planar applicators were designed with two quite different substrate heights (1.5 and 70 mm). The third design consisted of a MTM-ZOR resonator enclosed within a metal box structure having one open side facing the patient, thus resembling a waveguide applicator in appearance but not function. The next step towards practical use of these structures is to create antenna array configurations that allow heating large areas that are typical of chest wall recurrence of breast cancer, or alternatively to improve focused heating for deep tissue targets like pancreas or bladder.

In this paper, we introduce and characterize a novel MTM-ZOR array applicator. Furthermore we demonstrate the ability of this applicator to be arranged in several array configurations suitable for hyperthermia cancer treatment. We implement the characterization by means of finite element based numerical analysis using a proven commercial multiphysics simulation software: COMSOL Multiphysics (COMSOL AB, Stockholm, Sweden). Relative performance of the applicator arrays is compared with respect to homogeneity of power deposition and temperature induced in tissue-equivalent models of human muscle.

2. METHODS

2.1. Working Principles of Zeroth Order Mode Resonators

The equivalent circuit of a lossless MTM cell is shown in Fig. 1, where internal losses have been neglected for sake of simplicity. The MTM circuit is derived from an infinitesimally short lossless transmission line (TL) section described by a simple equivalent circuit, consisting of a series inductor L_R and a shunt capacitor C_R. The lossless MTM cell consists of a TL section with artificially inserted series capacitors C_L and shunt inductors L_L, where subscript L denotes its left-handed properties. The MTM cell equivalent circuit can be represented by four-lumped elements [12]. The working principle of ZOR is based on a special case of resonance that can occur when the TL (Fig. 1) meets one of the required conditions of MTM phenomenon. In Fig. 2(a), there is a relation between the phase constant β and frequency of the transmitted signal. The ZOR mode occurs when the frequency f corresponds to $\beta = 0$. This implies that the electrical length is equal to zero and the guided wavelength $\lambda_g = 2\pi/|\beta|$ is infinite along the MTM structure [1]. In Fig. 2(a), the dispersion diagram shows the positive resonances f_1, f_2 and f_3, corresponding to the classical $\lambda/2$, λ and $3\lambda/2$. The negative resonances f_{-1}, f_{-2}, f_{-3} are

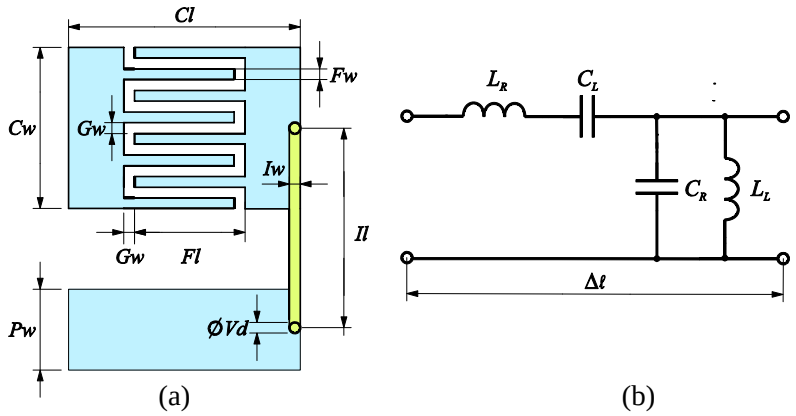

Figure 1. Building block element of MTM (a) and its equivalent circuit (b) consisting of inherent series inductance L_R and shunt capacitance C_R. Series capacitance C_L and shunt inductance L_L are created by the interdigitated capacitor and inductive stub, respectively.

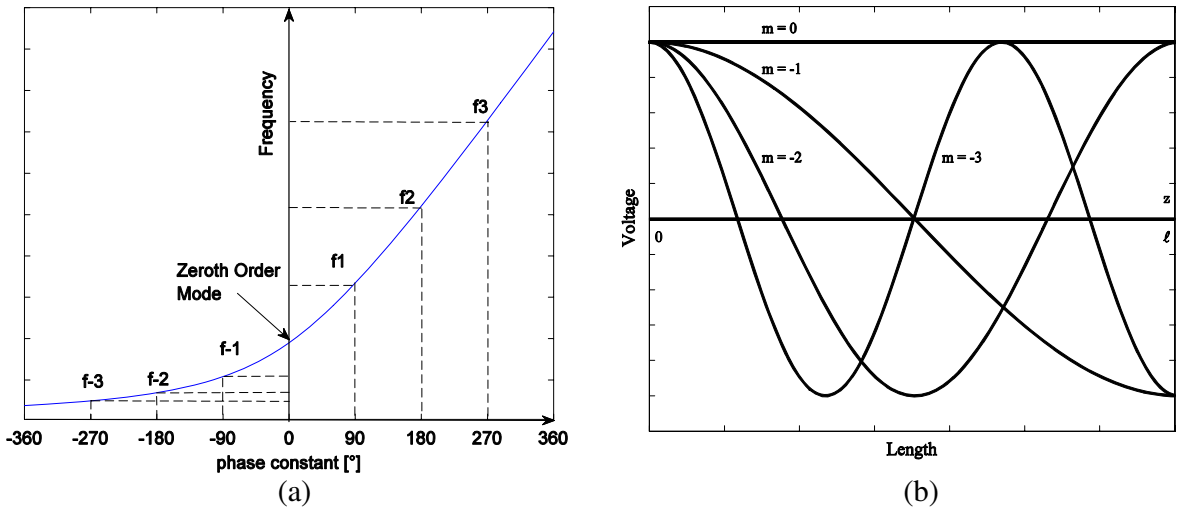

Figure 2. Relationship between electrical length and frequency f. Values of frequencies corresponding to resonance modes $m = -3, -2, \ldots, 2, 3$ are marked with $f_{-3}, f_{-2}, \ldots, f_{-2}, f_3$, (a). Voltage distribution in the case of an open-circuited TL section of length ℓ (b). Mode $m = 0$ represents the ZOR with infinite guided wavelength [1].

further depicted in Fig. 2(b), corresponding to the modes $m = -1$, $m = -2$ and $m = -3$ respectively. Since the Zeroth Order Mode is not dependent on the classical condition of resonance (multiple of half-wavelength), we can implement small radiating structures with high efficiency and whose physical length is independent of wavelength. Moreover, the ZOR mode shows another important property which we exploit here for homogeneous irradiation of the treated tissue: all MTM cells resonate in phase.

2.2. Design of MTM-ZOR Applicator

The first step in the applicator design is to estimate preliminary values of all equivalent circuit elements of a single MTM unit cell from Fig. 1. This includes initial estimates for the inductive radiating element dimensions, tuning capacitance, and dielectric constant of the substrate. The applicator design is then optimized via iterative numerical simulations, where the dimensions of TL's and interdigitated capacitors are modified in order to tune the ZOR structure to a working frequency of 434 MHz.

The MTM applicator investigated in this work is derived from an applicator design (type 1)

published in [16], which included a spatial asymmetry that generated an asymmetrical SAR pattern. The following modifications were performed in order to improve SAR symmetry and consequently increase temperature homogeneity as desired in hyperthermia treatments. First, the applicator was divided into two parts: TL feed and radiating element. The TL feed consists of a coaxial connector and an interdigitated capacitor (Fig. 3(b)), while the radiating element consists of four inductive bridges connected between 3 interdigitated capacitors and a grounded bar (Fig. 3(c)). The applicator was designed on a 2-layer dielectric substrate with a ground plane in the middle, which suppresses backside radiation from the applicator (Figs. 3(d) and 3(e)). The two parts are implemented on the two substrate layers and interconnected through a via hole in the ground plane, without touching ground.

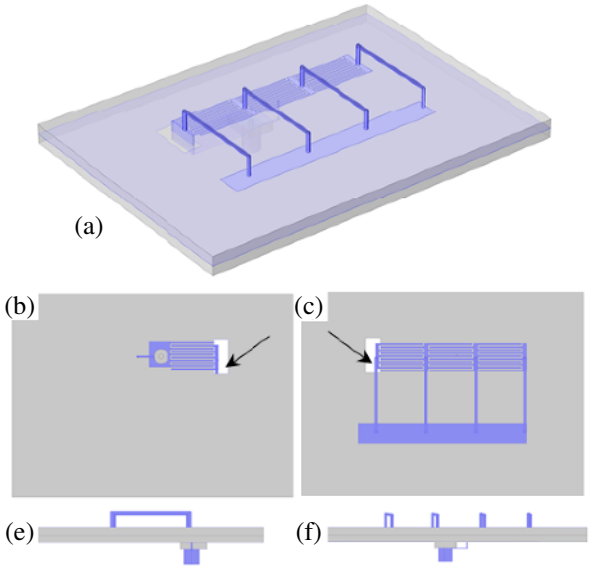

Figure 3. MTM-ZOR applicator design: 3D view (a); bottom view of the applicator showing the coaxial connector and the interdigitated capacitor placed on the back side of the applicator to maintain symmetry with the front radiating side (b); aperture view/front radiating side (c); side view showing the 5 mm thick substrates (gray) which extend above and below the central ground plane (d); and the inductive air bridges with 10 mm height above the substrate (e). White rectangles pointed by an arrow in (b) and (c) represent a rectangular hole in the ground plane.

The applicator is designed onFR4 substrate (model 370HR, Isola Group, Chandler AZ) with 5 mm height and relative permittivity $\varepsilon_r = 4.3$. The proposed applicator consists of 4 cells, where the overall length of one cell is $Cl = 34$ mm. The interdigitated capacitor width $Cw = 19$ mm consists of 10 fingers with length $Fl = 30$ mm; the finger width (Fw) and gap between fingers (Gw) is the same $Gw = Fw = 1$ mm; and the length of inductive components is $Il = 50$ mm. The interdigitated capacitor is connected to the referred ground pad (width $Pw = 13$ mm) by inductive air-bridges with width $Iw = 5$ mm. Due to the zeroth-order mode, currents flowing through the air bridges are approximately the same amplitude and phase and contribute significantly to the overall radiation pattern [1].

2.3. Applicator Performance

The applicator designs are evaluated in terms of Effective Field Size, here defined as the ratio of the are a enclosed by the 25% of maximum SAR contour in a given plane ($A_{\mathrm{SAR},25\%}$) divided by the footprint area of the radiating aperture (A_e).

$$EFS_{25} = \frac{A_{SAR,25\%}}{A_e} \tag{1}$$

The 25% of maximum SAR is generally considered to be the minimum power deposition required for effective heating of biological tissue without overheating tissue with the 100% SAR level. The EFS_{25}

was determined for planes 1, 2, and 3 cm deep in the homogeneous muscle tissue load. The SAR levels are normalized to the maximum SAR in the plane 1 cm below the surface.

The applicators are also characterized in terms of temperature distributions, using 2D cross section and 3D volume-based metrics, where we define therapeutic temperatures to be within the range of 41–45°C. We introduce the Therapeutic Thermal Area(TTA) as the 2D temperature metric, here defined as the ratio of area enclosed by the 41°C temperature contour in a given plane ($A_{T,41^\circ\mathrm{C}}$) divided by A_e.

$$TTA = \frac{A_{T,41^\circ C}}{A_e} \tag{2}$$

TTA is evaluated every 0.5 cm from the surface to 3.5 cm depth. Similarly, the Therapeutic Thermal Volume (TTV) is defined here as the ratio of volume enclosed within the 41°C contour in 1 cm thick slabs of tissue underlying the applicator ($V_{T,41^\circ\mathrm{C}}$) to the volume of the same 1 cm thick slabs circumscribed by the applicator aperture area (V_e).

$$TTV = \left.\frac{V_{T,41^\circ\mathrm{C}}}{V_e}\right|_{1\,\mathrm{cm}} \tag{3}$$

TTV is evaluated in volumes extending from the aperture surface to 1 cm depth, from1 to 2 cm depth, from 2 to 3 cm depth, and from 3 to 4 cm depth. Note that temperature is limited to 45°C maximum anywhere in muscle as a practical limit to avoid pain and undesirable toxicity in practical use.

2.4. Applicator Array Configurations

The wide variability of tumor size, shape and locations in the body requires a variety of different radiation patterns. Many superficial tumors cover large areas of the body, requiring large array configurations with adjustable shape heating patterns. In this paper we consider six different array configurations of the MTM-ZOR radiator: 1×1, 1×2, 2×1, 2×2, 2×3 and 3×2 (Fig. 4). Areas and dimensions of the multi-antenna arrays are listed in Table 1.

Table 1. Array arrangements and their dimensions.

Array arrangements	Figure	Dimensions (cm)	Aperture Area (cm^2)
1×1	4a	11.6×6.8	79
2×1	4b	24.6×6.8	167
1×2	4c	11.6×14.8	172
2×2	4d	24.6×14.8	364
2×3	4e	24.6×22.8	561
3×2	4f	37.6×14.8	556

2.5. Simulation Setup

The model consists of a 10 cm thick block of homogenous muscle phantom with a water compartment (bolus) of 1 cm thickness to enable circulation of water at a controlled temperature (T_{bolus}) to cool skin, minimize pain, and avoid excessive surface heating that might cause blisters. The water bolus also improves the coupling between applicator and tissue, thereby reducing reflections and leakage of microwave radiation at the applicator-tissue interface. Muscle and water dielectric properties are presented in Table 2 [17].

Temperature is simulated using the bioheat equation, introduced by Pennes in 1948 [18, 19] and is given by

$$\rho C_p \frac{\partial T}{\partial t} = \nabla \cdot (k \nabla T) + \omega_b C_{p,b} (T_a - T) + q_m + \rho SAR \tag{4}$$

Table 2. Dielectric properties used in the numerical models.

Dielectric properties at 434 MHz	FR4	De-ionized water (30°C)	De-ionized water (41°C)	Muscle tissue
ε_r	4.2	76.6	72.9	56.9
σ (S/m)	0.0016	0.00348	0.00257	0.81

where T is the tissue temperature, ρ density, C_p the specific heat capacity, k the thermal conductivity, ω_b the volumetric blood flow rate (kg/s/m^3), T_a the arterial blood temperature (37°C), q_m the metabolic heat source rate (W/m^3), and the index b stands for blood.

This equation is an expansion of the traditional heat equation to biological tissue, which accounts for the cooling effect of blood perfusion as a response to heating, metabolism, and also externally-induced EM heating. Both EM and heat transfer simulations are conducted in steady state conditions. The boundary condition between the water bolus and muscle is set to account for convection due to water flow with $h_{bolus} = 100\,\mathrm{W/m^2/K}$ [20] and $T_{bolus} = 30°\mathrm{C}$ or 41°C. The 30°C bolus temperature allows penetration of heat to somewhat deeper lying tumors while sparing surface tissue, whereas $T_{bolus} = 41°\mathrm{C}$ produces therapeutic heating including the skin surface as required for treating superficial chest wall recurrences [21]. The remaining outer boundaries of the muscle domain are set to account for convection losses to the environment, with $h_{air} = 5\,\mathrm{W/m^2/K}$ and $T_{air} = 25°\mathrm{C}$. Further parameters used for the bioheat equation are: specific heatof blood 3617 J/kg/K, blood density 1050 kg/m^3 and muscle metabolic heat rate 988 W/m^3. The traditional bioheat equation assumes constant blood perfusion, but this important thermoregulatory function varies during heat treatment as a function of both temperature and time. Two blood perfusion values were investigated to account for the lower and upper limits: 0.75 kg/s/m^3 to mimic basal blood perfusion of muscle [19] and 5.0 kg/s/m^3 to simulate the higher blood perfusion typical of heated normal muscle [22].

3. RESULTS

One of the goals of this work is to investigate how to combine multiple MTM-ZOR radiators into arrays that heat large areas contiguously without gaps. To achieve this goal we have performed a parametric study using different dimensions (C_L, F_L, F_W, G_w, I_w, P_w, C_w) of a single antenna applicator, as well as different spacings between the antennas of the array. The spacings have been tested iteratively in both dimensions with steps of 1 mm. As a result, the best homogeneity of power deposition was achieved for spacings corresponding to 14 mm and 10 mm in the X and Y axes, respectively. Subsequently, this optimal spacing was used during the evaluation of all antenna array configurations.

The normalized SAR patterns are presented in Fig. 4 for all arrays listed in Table 1. The 50% SAR contour level is roughly achieved over the antenna aperture and the 25% contour extends several centimeters beyond the aperture. Fig. 5 shows the EFS_{25} at three different depths in the homogeneous muscle model. EFS_{25} is almost 190% of the aperture area at 1 cm depth for both the single antenna (black) and 2×2 array (yellow), but the relative performance diverges with increasing depth such that the 2×2 array reaches much higher EFS_{25} (100%) at 3 cm depth than the single antenna (69%). The 2×3 array applicator (blue) EFS_{25} profile is flatter than the other two cases: at 1 cm depth it achieves 138% which falls only to 91% at 3 cm depth. This indicates a trend toward higher directivity with larger numbers of antennas in the array.

Figures 6 and 7 show temperature simulations in muscle under the array applicators. Fig. 6 displays the temperature distribution for the 2×3 array with water bolus temperature of 30°C and blood perfusion of 0.75 kg/s/m^3. The temperature varies from 43.4 to 44.9°C at 2 cm depth, and from 42.4–43.2°C in the 3.5 cm deep plane, for a maximum temperature of 45°C anywhere in tissue.

Figure 8 presents the Therapeutic Thermal Area (TTA) given in 8 different planes from the surface to 3.5 cm depth. Fig. 8(a) shows the metamaterial applicator performance with 30°C water bolus cooling; the TTA remains above 86% to a depth of 3.5 cm for the 2×2 and 2×3 array applicators. In the case of 41°C water bolus temperature, the desired 41°C minimum treatment temperature extends up to the

tissue surface, but TTA tapers off below 85% by 3 cm depth (Fig. 8(b)) for all array configurations. Fig. 9 shows the analogous profiles for a high perfusion level of 5.0 kg/s/m^3. As expected, the temperature falls off more rapidly with depth at this much higher perfusion level. For the 41°C bolus, the TTA falls below 40% for all applicator sizes by 2.5 cm depth. Even with the increased cooling of surface tissues with 30°C bolus, the TTA falls below 44% by 2.5 cm depth for all but the largest 2×3 array.

As shown in Fig. 10, assuming basal blood perfusion (0.75 kg/s/m^3) the tissue volume heated within the therapeutic range 41–45°C (TTV) includes 90–130% of the 1 cm thick slab volume contained between X and $(X-1)$ bounded by the aperture perimeter to a depth of 3 cm, and at least 50% of the volume remains in the therapeutic range to 4 cm depth. For highly perfused tissue (5.0 kg/s/m^3), the TTV falls off more quickly, with almost 90% of the slab volume in the therapeutic range at 2 cm depth falling to $< 60\%$ at 3 cm and 0% at 4 cm depth.

4. DISCUSSION

We present a characterization of different metamaterial antenna arrays based on a novel MTM-ZOR antenna design. We used three different metrics to demonstrate the potential of these applicator arrays for the field of microwave hyperthermia. One metric quantified SAR patterns that are proportional to the antenna radiation pattern in a homogeneous muscle tissue load, one metric quantified 2D temperature distributions in several planes at depth in perfused tissue, and one metric quantified the percentage of tissue volume that falls within the therapeutic temperature range of 41–45°C in 1 cm thick slabs of perfused tissue underlying the applicators. In order to study metamaterial antenna arrays that can heat large tissue regions, the single aperture MTM-ZOR antenna design described in [12] was modified to facilitate combination with adjacent apertures. This modified antenna produced an improvement in

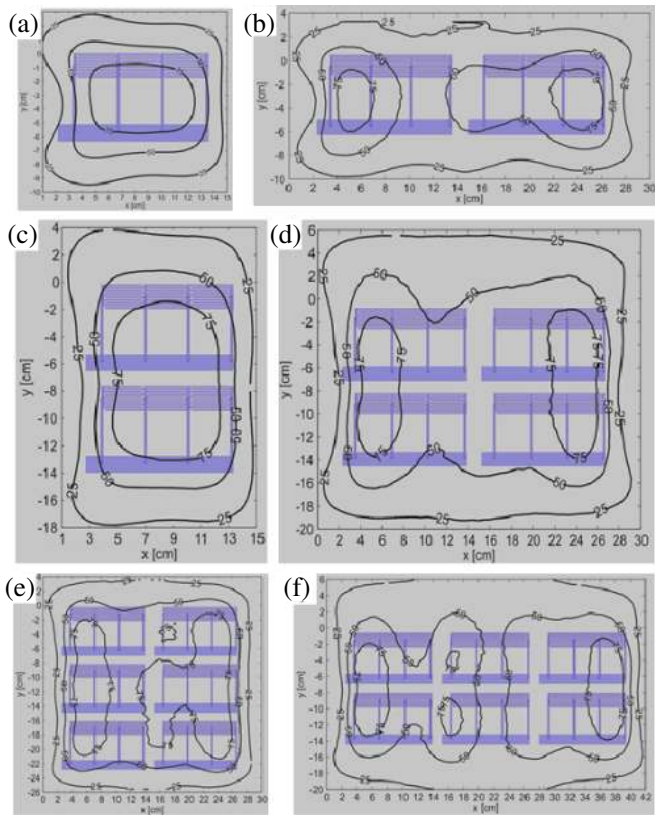

Figure 4. SAR patterns at 1 cm depth in muscle tissue under six MTM-ZOR antenna array configurations. The contours correspond to 25, 50 and 75% SAR percentiles normalized to the SAR maximum in the 1 cm deep plane.

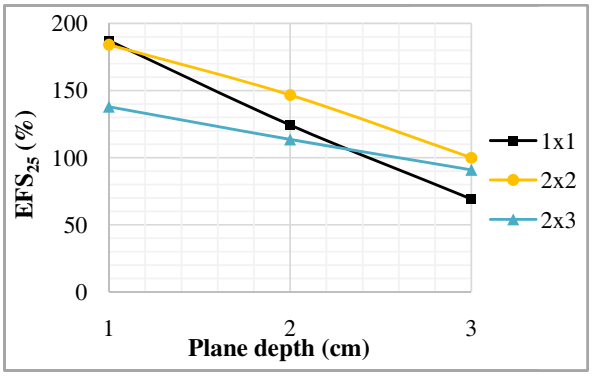

Figure 5. Comparison of EFS_{25} at 1, 2 and 3 cm depths for three applicator array configurations.

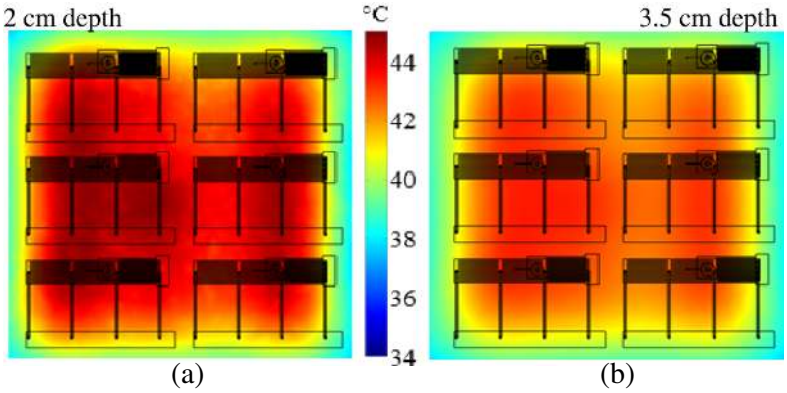

Figure 6. Temperature distribution at 2 cm (a) and 3.5 cm depth (b) under the 3×2 aperture array with $T_{bolus} = 30°C$, $b = 0.75\,kg/s/m^3$ and $P_{ant} = 60\,W$. The yellow color denotes the threshold therapeutic temperature of 41°C.

EFS_{25} at 1, 2, and 3 cm depths over the initial design of 28%, 17%, and 13% respectively. The EFS_{25} at 3 cm depth under the original applicator was 56% while EFS_{25} of the modified applicator is 69%.

MTM applicators, studied and described in this paper, are composed of a matrix ($m \times n$ elements) of ZOR structures, each of them radiating EM waves that are nearly plane wave in structure. Since we are interested in obtaining homogeneous heating of the entire treated area, the superposition of fields radiated from all ZOR structures should approximate plane wave as well. For the array geometries analyzed (Fig. 4), the contiguous treatment areas are regular in shape — generally square or rectangular. In the clinic, tumor shapes and areas to be treated are usually more complex. To get the best possible fit of the area treated by an MTM array with $m \times n$ ZOR elements, it is possible to adjust the shape of the heating pattern by varying relative power to each of the ZOR structures and/or turning off excitation to elements that are not adjacent to tumor target. In this way, the SAR distribution is tailored to most effectively heat tumor tissue while minimizing heating of surrounding healthy tissue.

During our investigation of array configurations, we initially assumed that the symmetry of power deposition patterns would be improved by using mutually symmetric adjacent antennas. Fortunately, this hypothesis was not confirmed and the SAR patterns generated by symmetric and asymmetric array designs are similarly effective. Thus, array configurations are not in general limited with respect to the number of antennas.

In order to produce effective well-localized heating under an applicator, a similar EFS_{25} is desired at all target depths. In Fig. 5, we observe that the slope of EFS_{25} with depth is flatter (i.e., more consistent SAR coverage at all depths) for the larger multi-antenna arrays. This is verified with thermal simulations that show the 2×2 and 2×3 arrays provide more similar heating profiles at all depths than the smaller

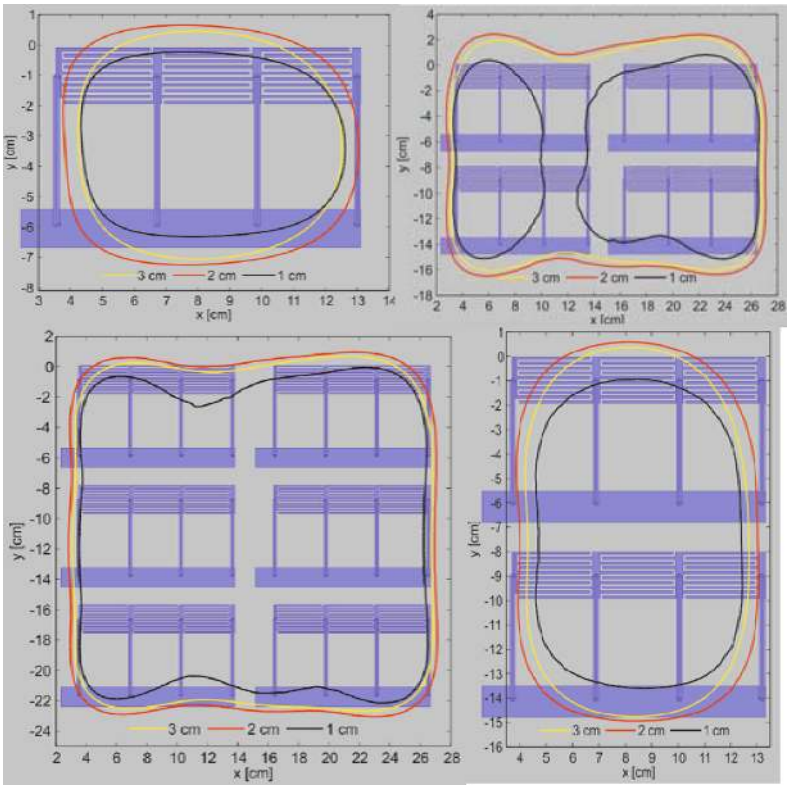

(a) (b)

Figure 7. 41°C temperature contour at a depth of 1 cm (black), 2 cm (red) and 3 cm (yellow) in 1×1, 2×2, 3×2, and 1×2 applicator configurations. $T_{bolus} = 30$°C, $b = 0.75\,\mathrm{kg/s/m^3}$ and $P_{ant} = 40\,\mathrm{W}$ (1×1). In the whole computational domain temperature did not exceed 45°C.

1×1 and 1×2 arrays (Figs. 6–10).

An important characteristic of these MTM applicators is the fact that surface currents have the same amplitude and phase on all air bridges. These surface currents are the primary source of radiation from the MTM applicators. This coherent combination of drive currents maximizes irradiation of tissue directly below the aperture, in a manner similar to a plane wave radiation. However, the propagating EM wave changes from plane wave to a more spherical polarization with increasing distance from the aperture. The region of quasi-plane wave is larger for larger array configurations. In agreement with the Huygens principle, there is radiation in directions other than the direction perpendicular to the aperture. This off axis radiation is responsible for EFS_{25} larger than 100% at 1 cm depth presented in Figs. 4 and 5.

Figure 7 shows that despite having an EFS_{25} much larger than 100%, the 41°C contours in 1, 2 and 3 cm deep planes surround areas that are smaller than the aperture area for 1×1 and 1×2 configurations. Fortunately, the 41°C contours are comparable to the aperture dimensions for the 2×2 and 3×2 arrays. It is also clear from Figs. 6 and 7 that the tissue surrounding the aperture is cooled effectively by the water bolus so there are no hot spots between or outside the apertures.

Two water bolus temperatures were used to simulate different treatment scenarios. To treat superficial tumors involving the tissue surface, we used a bolus temperature of 41°C which produced a therapeutic temperature range from the surface down to 2.5 cm depth for the larger 2×2 and 2×3 array applicators. To treat deeper tumors not involving the top 5–10 mm of tissue, it is appropriate to use a lower temperature — of the order 30°C — to cool the surface and increase penetration of effective heating. In this case, therapeutic temperatures were achieved as deep as 3.5 cm. The effect of surface cooling is further depicted in Fig. 7, which shows that the 41°C temperature contour at 2 cm depth (red curve) covers a larger area than at 1 and 3 cm.

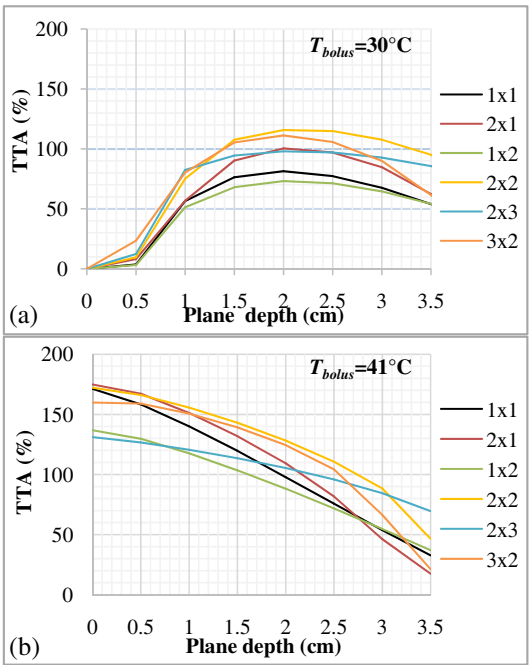

Figure 8. Dependence of TTA temperature on penetration depth for six applicator configurations for different water bolus temperature: T_{bolus} = 30°C. (a) and T_{bolus} = 41°C. (b) ω_b = 0.75 kg/s/m^3.

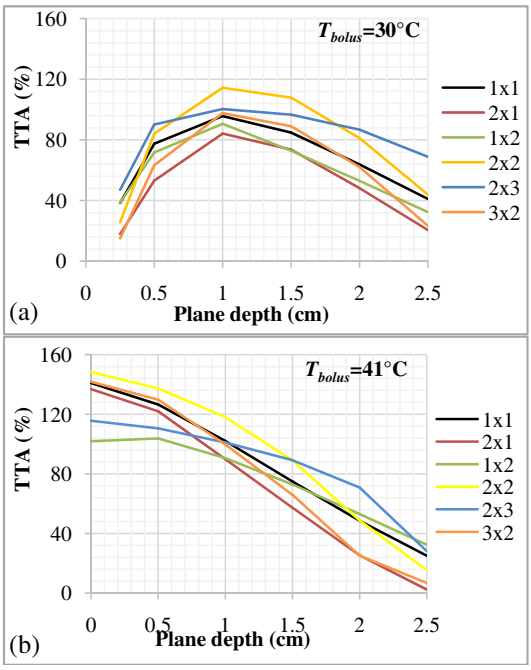

Figure 9. Dependence of TTA temperature on penetration depth for six applicator configurations for different water bolus temperature: T_{bolus} = 30°C. (a) and T_{bolus} = 41°C. (b) ω_b = 5.0 kg/s/m^3.

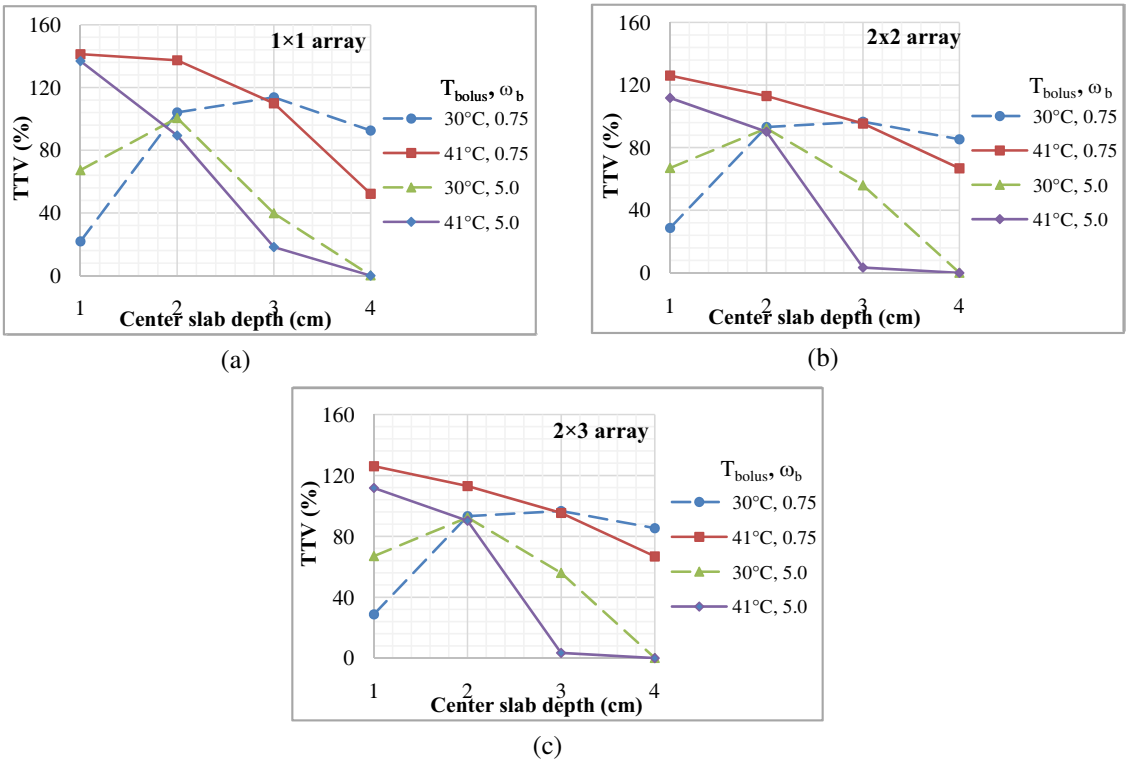

Figure 10. Dependence of TTV_{41} temperature for one antenna (a); 2 × 2 array (b); and 2 × 3 array, (c) for different water bolus temperatures and tissue perfusions in kg/s/m^3.

Blood perfusion is dependent not only on temperature but also on heating time. The temperature dependence is not linear and blood perfusion can reach values as high as $5.0\,\mathrm{kg/s/m^3}$ in muscle during hyperthermia treatments [22]. The purpose of this work is not to provide treatment planning for a specific patient but rather to characterize the performance of hyperthermia applicators possible over a typical range of blood perfusion. Thus, we present a study of heating patterns possible at the lower ($0.75\,\mathrm{kg/s/m^3}$) and upper limits ($5\,\mathrm{kg/s/m^3}$) of blood perfusion in muscle tissue.

The blood perfusion in superficial tumors during hyperthermia was studied by Waterman et al. [23]. They characterized perfusion in 1–3 cm deep tumors such as melanomas, squamous cell carcinomas and adenocarcinomas at temperatures ranging from 41.7–45.0°C. They reported that tumor blood perfusion was in the same range as muscle during hyperthermia [22], which allows us to extrapolate the conclusions of our present study to cover typical superficial tumors, i.e., our applicators should be able to effectively heat superficial tumors.

5. CONCLUSIONS

This paper investigates the heating performance of novel multi-element array hyperthermia applicators based on a metamaterial zeroth order mode antenna. This particular antenna is suitable for assembly into large array applicators that are shown to provide more homogenous heating (41–45°C) of large target areas than possible with typical waveguide antennas. These applicators can heat effectively down to 3–4 cm depth using a water bolus temperature of 30°C with moderate or high level blood perfusion. The applicator performance is characterized with three metrics, the EFS is a standard metric, but both the Therapeutic Thermal Area (TTA) and Therapeutic Thermal Volume (TTV) are here introduced and proved to be adequate for a more in depth characterization of hyperthermia applicators. The EFS_{25} in the 3 cm deep plane of 2×2 and 2×3 arrays reached 100% and 91%, respectively. The TTA for these two arrays was 95% and 86% in the 3.5 cm deep plane. The TTV reached almost 100% to a depth of 2 cm at high perfusion and about 80% to a depth of 4 cm in moderate perfusion. The data demonstrate that these metamaterial antenna array applicators can uniformly heat large areas of tissue up to $560\,\mathrm{cm^2}$. By further increasing the number of antennas, it should be possible to treat even larger disease to therapeutic temperatures from 41–45°C.

ACKNOWLEDGMENT

This research has been supported by the research program of the Czech Scientific Foundation, project No. 14-00386P and by EU project COST action TD1301.

REFERENCES

1. Caloz, C. and T. Itoh, *Electromagnetic Metamaterials: Transmission Line Theory and Microwave Applications: The Engineering Approach*, John Wiley & Sons, New Jersey, 2006.
2. Cihoric, N., A. Tsikkinis, G. van Rhoon, H. Crezee, D. M. Aebersold, S. Bodis, M. Beck, J. Nadobny, V. Budach, P. Wust, and P. Ghadjar, "Hyperthermia-related clinical trials on cancer treatment within the Clinical Trials. gov registry," *International Journal of Hyperthermia*, Vol. 31, No. 6, 609–614, May 2015.
3. Dewhirst, M. W., Z. Vujaskovic, E. Jones, and D. Thrall, "Re-setting the biologic rationale for thermal therapy," *International Journal of Hyperthermia*, Vol. 21, No. 8, 779–790, Dec. 2005.
4. Sneed, P. K., P. R. Stauffer, G. Li, X. Sun, and R. Myerson, "Hyperthermia," *Textbook of Radiation Oncology*, 3rd Edition, T. Phillips, R. Hoppe, and M. Roach, eds., 1564–1593, Elsevier Saunders Co, Philadelphia, 2010.
5. Paulides, M. M., P. R. Stauffer, E. Neufeld, P. F. Maccarini, A. Kyriakou, R. A. Canters, C. J. Diederich, J. F. Bakker, and G. C. van Rhoon, "Simulation techniques in hyperthermia treatment planning," *International Journal of Hyperthermia*, Vol. 29, No. 4, 346–357, Jun. 2013.
6. Veselago, V., "The electrodynamics of substances with simultaneously negative values of ε and μ," *Sov. Phys. Usp.*, Vol. 10, No. 4, 509–514, 1968 (Russian text 1967).

7. Shelby, R. A., D. R. Smith, and S. Schultz, "Experimental verification of a negative index of refraction," *Science*, Vol. 292, No. 5514, 77–79, Apr. 6, 2001.
8. Vrba, D. and M. Polivka, "Radiation efficiency improvement of zeroth-order resonator antenna," *Radioengineering*, Vol. 18, No. 1, 1–8, Apr. 2009.
9. Polivka, M. and D. Vrba, "Shielded micro-coplanar CRLH TL zeroth-order resonator antenna: Critical performance evaluation," *Radioengineering*, Vol. 18, No. 4, 368–372, Dec. 2009.
10. Wang, G. and Y. Gong, "Metamaterial lens applicator for microwave hyperthermia of breast cancer," *International Journal of Hyperthermia*, Vol. 25, No. 6, 434–445, 2009.
11. Leggio, L., O. de Varona, and E. Dadrasnia, "Comparison between different schemes of microwave cancer hyperthermia treatment by means of left-handed metamaterial lenses," *Progress In Electromagnetics Research*, Vol. 150, 73–87, 2015.
12. Vrba, D. and J. Vrba, "Novel applicators for local microwave hyperthermia based on zeroth-order mode resonator metamaterial," *International Journal of Antennas and Propagation*, Vol. 2014, 1–7, 2014.
13. Lee, E. R., T. R. Wilsey, P. Tarczyhornoch, D. S. Kapp, P. Fessenden, A. Lohrbach, and S. D. Prionas, "Body conformable 915 MHz microstrip array applicators for large surface-area hyperthermia," *IEEE Transactions on Biomedical Engineering*, Vol. 39, No. 5, 470–483, May 1992.
14. Johnson, J. E., D. G. Neuman, P. F. Maccarini, T. Juang, P. R. Stauffer, and P. Turner, "Evaluation of a dual-arm Archimedean spiral array for microwave hyperthermia," *International Journal of Hyperthermia*, Vol. 22, No. 6, 475–490, Sep. 2006.
15. Rieke, V. and K. B. Pauly, "MR thermometry," *Journal of Magnetic Resonance Imaging*, Vol. 27, No. 2, 376–390, Feb. 2008.
16. Vrba, D., J. Vrba, and P. Stauffer, "Novel microwave applicators based on zero-order mode resonance for hyperthermia treatment of cancer," *Proceedings of the IEEE BenMAS 2014*, 107–109, Sep. 2014.
17. Ellison, W. J., "Permittivity of pure water, at standard atmospheric pressure, over the frequency range 0–25 THz and the temperature range 0–100 degrees C," *Journal of Physical and Chemical Reference Data*, Vol. 36, No. 1, 1–18, Mar. 2007.
18. Pennes, H. H., "Analysis of tissue and arterial blood temperatures in the resting human forearm," *Journal of Applied Physiology*, Vol. 1, 93–122, 1948.
19. Hasgall, P. A., F. Di Gennaro, E. Neufeld, M. C. Gosselin, D. Payne, A. Klingenböck, and N. Kuster, "IT'IS Database for thermal and electromagnetic parameters of biological tissues, Version 2.6," Jan. 13, 2015.
20. Van der Gaag, M. L., M. de Bruijne, T. Samaras, J. van der Zee, and G. C. van Rhoon, "Development of a guideline for the water bolus temperature in superficial hyperthermia," *International Journal of Hyperthermia*, Vol. 22, No. 8, 637–656, Dec. 2006.
21. Stauffer, P. R., P. Maccarini, K. Arunachalam, O. Craciunescu, C. Diederich, T. Juang, F. Rossetto, J. Schlorff, A. Milligan, J. Hsu, P. Sneed, and Z. Vujaskovic, "Conformal microwave array (CMA) applicators for hyperthermia of diffuse chest wall recurrence," *International Journal of Hyperthermia*, Vol. 26, No. 7, 686–986, Oct. 2010.
22. Sekins, K. M., J. F. Lehmann, P. Esselman, D. Dundore, A. F. Emery, B. J. Delateur, and W. B. Nelp, "Local muscle blood-flow and temperature responses to 915 MHz diathermy as simultaneously measured and numerically predicted," *Archives of Physical Medicine and Rehabilitation*, Vol. 65, No. 1, 1–7, Jan. 1984.
23. Waterman, F. M., R. E. Nerlinger, D. J. Moylan, and D. B. Leeper, "Response of human tumor blood flow to local hyperthermia," *International Journal of Radiation Oncology Biology Physics*, Vol. 13, No. 1, 75–82, Jan. 1987.